

Supporting Information for:

Macrocyclic ligand encapsulating dysprosium triangles: axial ligands perturbed magnetic dynamics

Experimental Section

General. All starting materials were of A.R. Grade and were used as commercially obtained without further purification. 2, 6-diformyl-4-methylphenol (DFMP) and H₃L were prepared according to a previously published method.^{1,2}

Elemental analyses for C, H, and N were carried out on a Perkin-Elmer 2400 analyzer. Fourier transform IR (FTIR) spectra were recorded with a Perkin-Elmer FTIR spectrophotometer using the reflectance technique (4000–300 cm⁻¹). Samples were prepared as KBr disks. All magnetization data were recorded on a Quantum Design MPMS-XL7 SQUID magnetometer equipped with a 7 T magnet. The variable-temperature magnetization was measured with an external magnetic field of 1000 Oe in the temperature range of 1.9–300 K. The experimental magnetic susceptibility data are corrected for the diamagnetism estimated from Pascal's tables and sample holder calibration.

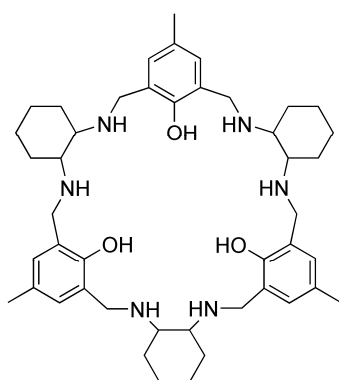
Synthesis of [Dy₃L(μ₃-OH)₂(NO₃)₂(H₂O)₄]·2NO₃·6CH₃OH·H₂O (**1**). A solution of H₃L (0.05 mmol) in methanol (15 mL) was added Et₃N (0.2 mmol) and Dy(NO₃)₃·6H₂O (0.2 mmol, 91.32 mg). The reaction mixture was stirred at room temperature for 2 h and the resultant solution was left unperturbed to allow for slow evaporation of the solvent. Colourless single crystals of complex **1** were obtained after a few days. Yield: 15 mg, (13 %, based on the metal salt). Elemental analysis (%) calcd for Dy₃C₅₁H₉₉N₁₀O₂₈: C, 34.26, H, 5.58, N, 7.83; found C, 33.98, H, 5.13, N, 7.51. IR (KBr, cm⁻¹): 3564 (w), 3245 (w), 2933 (m), 2859 (w), 1469 (s), 1450 (s), 1312 (s), 1252 (s), 1221 (m), 1168 (m), 1033 (m), 1016 (m), 954 (w), 887 (w) 795 (m), 567 (w).

Synthesis of [Dy₃L(μ₃-OH)₂(SCN)₄(H₂O)₂]·3CH₃OH·2H₂O (**2**). A solution of H₃L (0.05 mmol) in a mixed solvent of methanol (10 mL) and dichlormethane (10 mL) was added KOH (0.2 mmol) and Dy(SCN)₃·6H₂O (0.2 mmol). The reaction mixture was stirred at room temperature for 2 h and the resultant solution was left unperturbed to allow for slow evaporation of the solvent. Colourless single crystals of complex **2** were obtained after a few days. Yield: 18 mg, (16 %, based on the metal salt). Elemental analysis (%) calcd for C₅₂H₈₅Dy₃N₁₀O₁₂S₄: C, 37.67, H, 5.17, N, 8.45; found C, 37.32, H, 4.86, N, 8.24. IR (KBr, cm⁻¹): 3354 (br), 3267 (w), 2934 (m), 2859 (w), 2058 (s), 1618 (w), 1467 (s), 1255 (m), 1244 (m), 1169 (w), 1091 (w), 884 (w), 842 (w), 769 (m), 657 (br), 483 (w).

X-ray Crystallography. Crystallographic data and refinement details are given in Table S1. Suitable single crystal of **1** was selected for single-crystal X-ray diffraction analysis. Crystallographic data were collected at 185(2) K on a Bruker ApexII CCD diffractometer with graphite monochromated Mo Kα radiation ($\lambda = 0.71073 \text{ \AA}$). The structure was solved by direct methods and refined on F^2 with full-matrix least-squares techniques using SHELXS-97 and SHELXL-97 programs.^{3,4} The locations of Dy atom were easily determined, and O, N, C and S atoms were subsequently determined from the difference Fourier maps. Anisotropic thermal parameters were assigned to all non-hydrogen atoms. The H atoms were introduced in calculated positions and refined with a fixed geometry with respect to their carrier atoms. CCDC 871485 (**1**) and 871486 (**2**) contain the supplementary crystallographic data for this paper. These data can be obtained free of charge from the Cambridge Crystallographic Data Centre via www.ccdc.cam.ac.uk/data_request/cif.

References:

1. R. R. Gagne, C. L. Spiro, T. J. Smith, C. A. Hamann, W. R. Thies and A. K. Shiemke, *J. Am. Chem. Soc.*, 1981, **103**, 4073-4081.
2. J. Gao, R. A. Zingaro, J. H. Reibenspies and A. E. Martell, *Org. Lett.*, 2004, **6**, 2453-2455.
3. G. M. Sheldrick, *SHELXS-97, Program for Crystal Structure Solution*, University of Göttingen, Germany, 1997.
4. G. M. Sheldrick, *SHELXL-97. Program for Crystal Structure Refinement*, University of Göttingen, Germany, 1997.



Scheme S1. Structure of the H₃L ligand.

Table S1 Crystal data and structure refinement for complex **1** and **2**.

Compound	1	2
Empirical formula C ₅₁ H ₉₉ Dy ₃ N ₁₀ O ₂₈ C ₅₂ H ₈₅ Dy ₃ N ₁₀ O ₁₂ S ₄		
Fw (g/mol)	1787.90	1658.04
Crystal system	Triclinic	Monoclinic
Space group	<i>P</i> $\bar{1}$	<i>P</i> 2(1)/ <i>n</i>
Crystal colour	colourless	colourless
<i>a</i> (Å)	14.833(2)	16.9137(12)
<i>b</i> (Å)	16.5643(12)	16.8688(12)
<i>c</i> (Å)	16.5770(12)	29.163(2)
α (°)	119.774(1)	90
β (°)	100.183(1)	90.316(1)
γ (°)	90.507(1)	90
<i>V</i> (Å ³)	3457.3(6)	8320.6(10))
ρ_{calcd} (Mg/m ³)	1.717	1.324
<i>F</i> (000)	1794	3300
<i>R</i> _{int}	0.0270	0.0779
<i>R</i> ₁ , <i>wR</i> ₂ [<i>I</i> > 2σ(<i>I</i>)]	0.0425, 0.1033	0.0804, 0.2230
<i>R</i> ₁ , <i>wR</i> ₂ (all data)	0.0639, 0.1224	0.1408, 0.2578
GOF	1.067	1.046

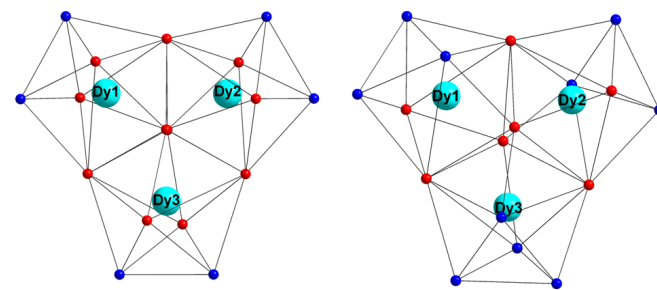


Fig. S1 Coordination polyhedra observed in complex **1** (left) and **2** (right).

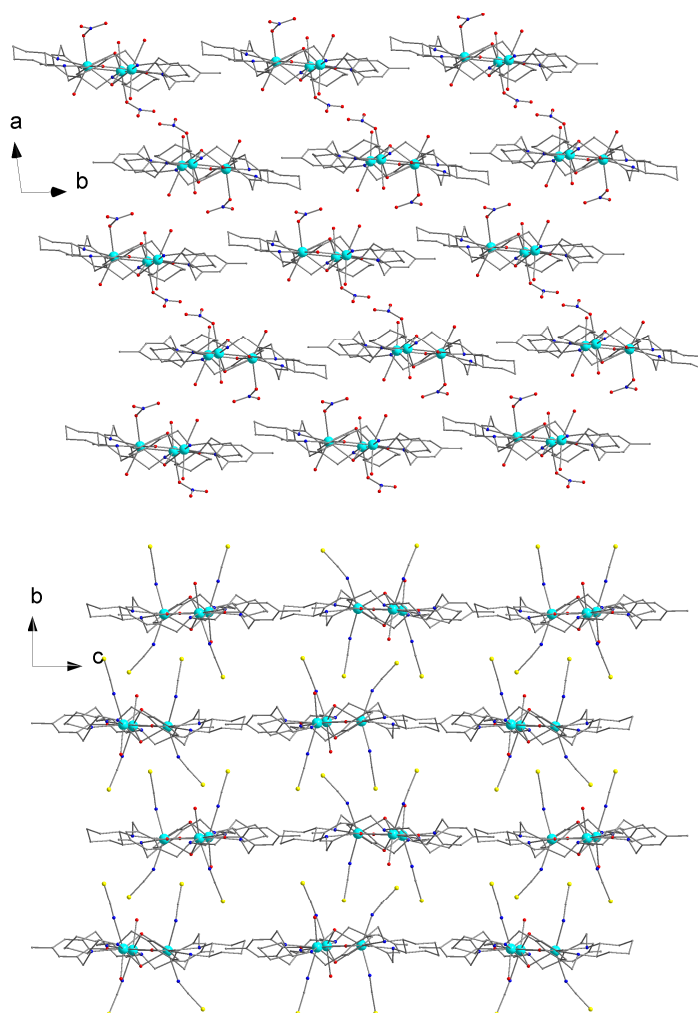


Fig. S2 Crystal packing of complex **1** (top) and **2** (bottom) along *c* and *a* axis, respectively.

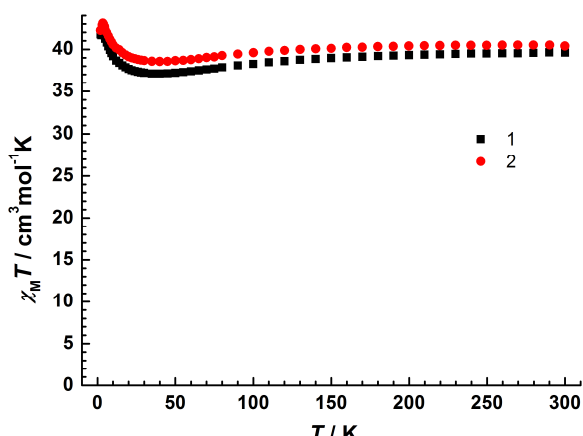


Fig. S3 Temperature dependence of the $\chi_M T$ product for **1** and **2**.

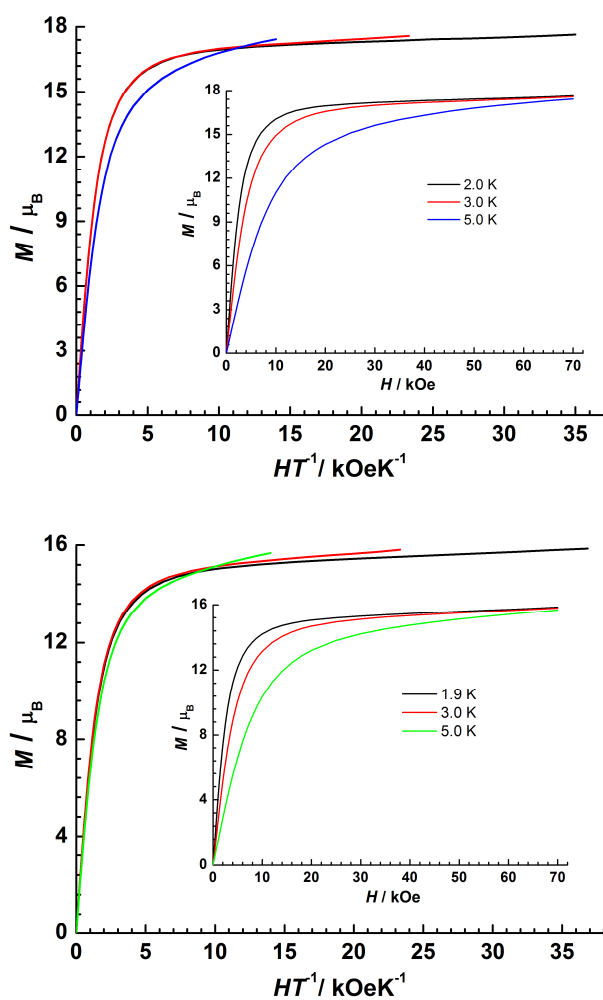


Fig. S4 Plots of the reduced magnetization M vs. H/T in the field range 0-70 kOe and temperature range 1.9-5.0 K.
Inset: Field dependence of the magnetization. Top for **1**, bottom for **2**.

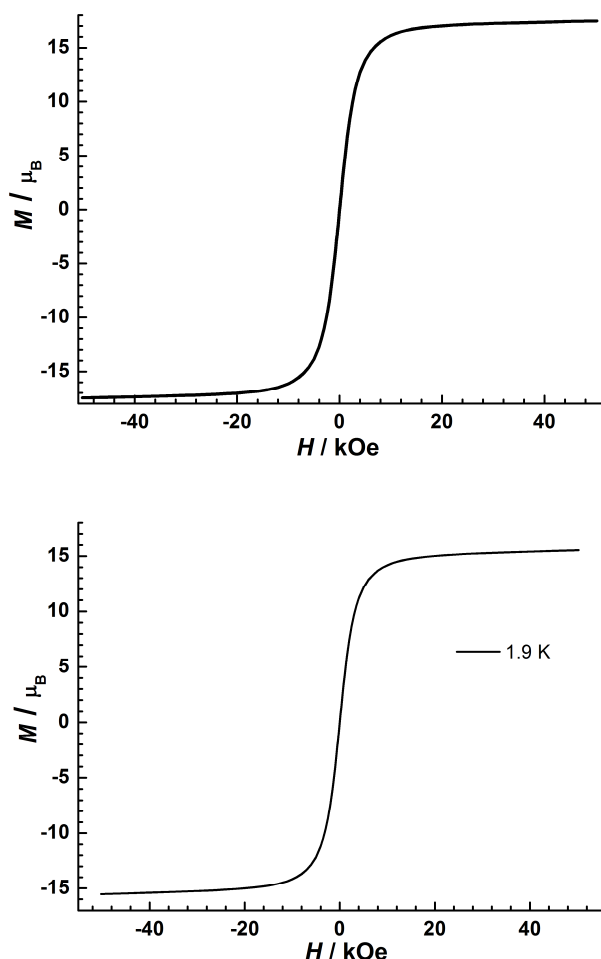


Fig. S5 Hysteresis loop for complex **1** (top) and **2** (bottom) at 1.9 K.

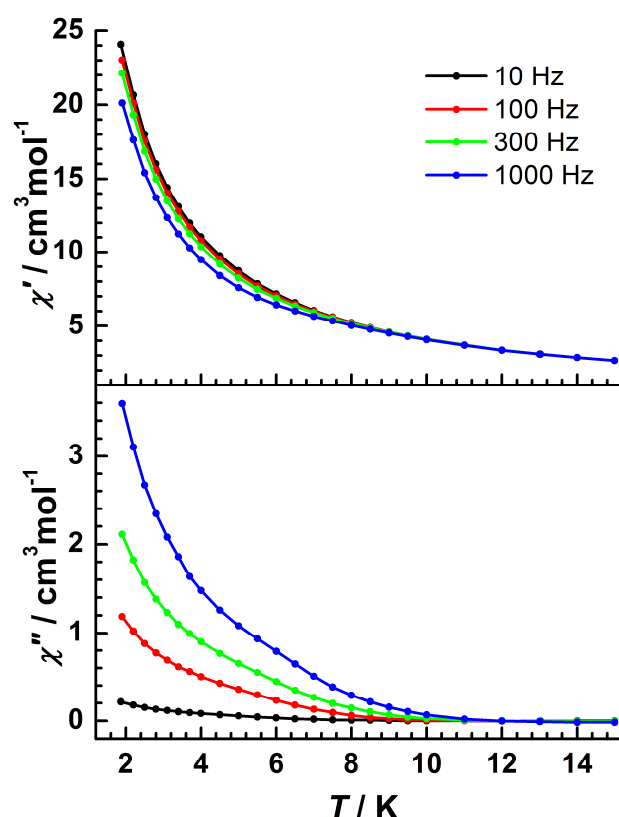


Fig. S6 Temperature- dependence of the ac susceptibility under zero dc field for **1**. The solid lines are guides for the eyes.

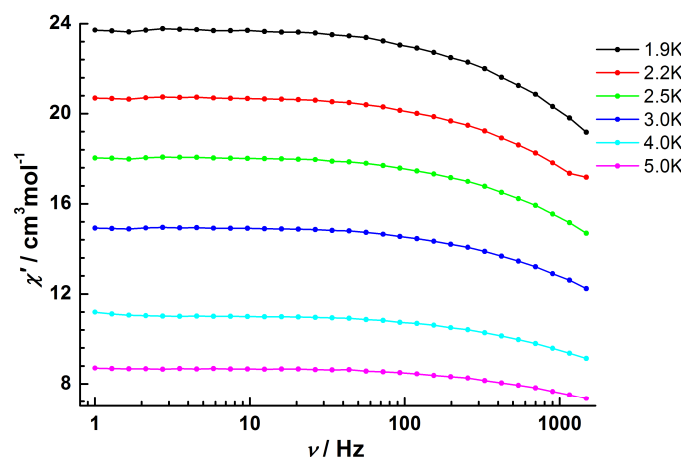


Fig. S7 Frequency- dependences of χ' of **1** measured under zero dc field.

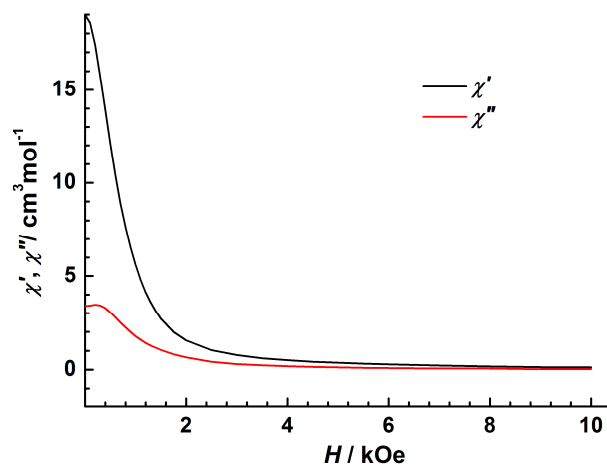


Fig. S8 Field-dependent ac susceptibility of **1** measured at 1.9 K and 1000 Hz.

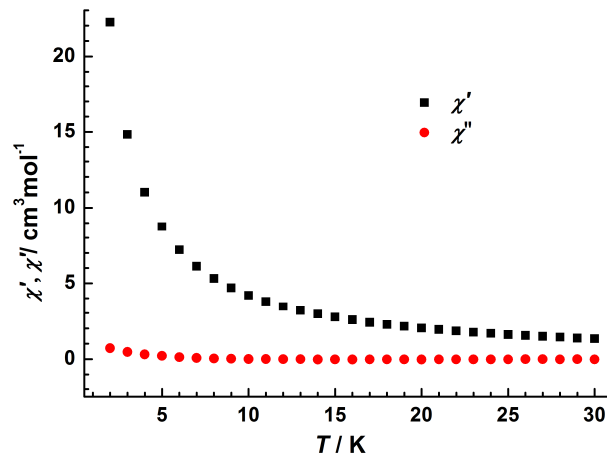


Fig. S9 Temperature dependence of χ' (black) and χ'' (red) for **2** measured at 1000 Hz under zero dc field.

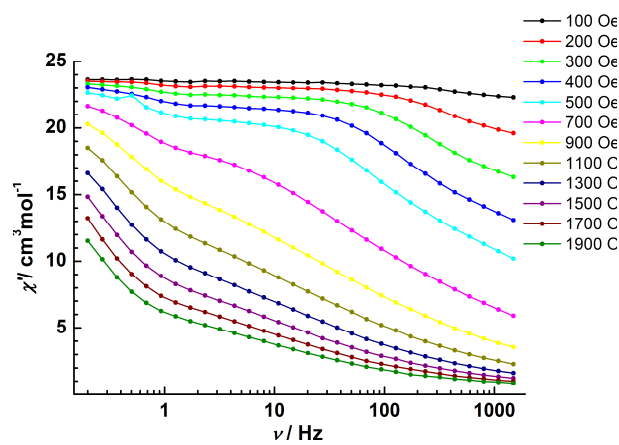


Fig. S10 Frequency dependence of the in-phase ac susceptibility under various applied fields at 1.9 K for **2**. The solid lines are guides for the eyes.

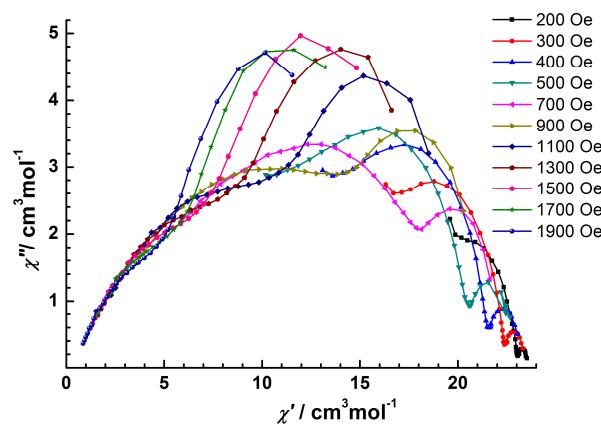


Fig. S11 Cole-Cole plots under variable static fields at 1.9 K for **2**. Two asymmetric semicircles are evident in the range 400–1100 Oe.

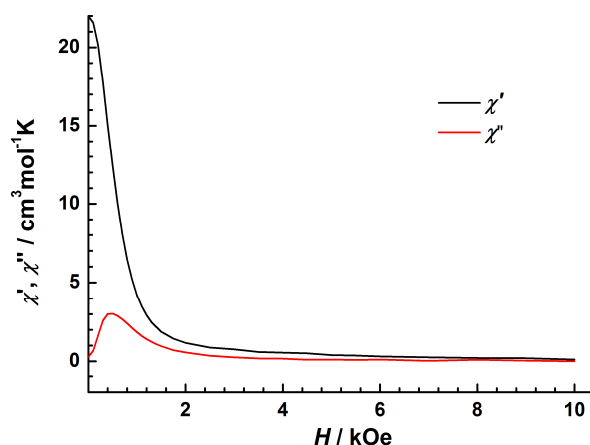


Fig. S12 Field- dependent ac susceptibility measured at 1.9 K and 1000 Hz for **2**. χ'' signal with a significant peak around 500 Oe dc field indicates field-enhanced slow magnetic relaxation operating in **2**.

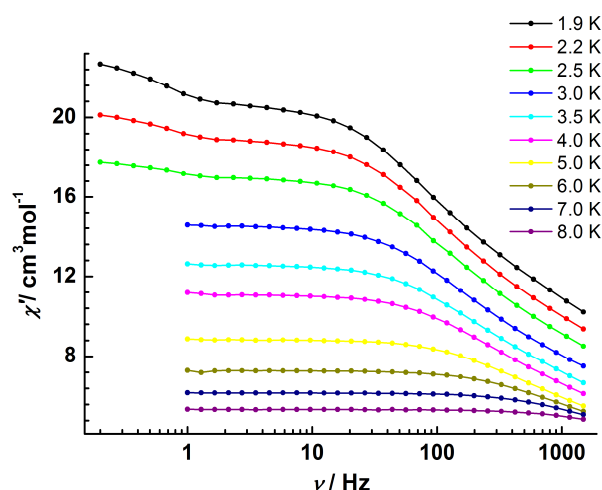


Fig. S13 Frequency- dependence of the in-phase ac susceptibility under 500 Oe dc field for **2**. The solid lines are guides for the eyes.

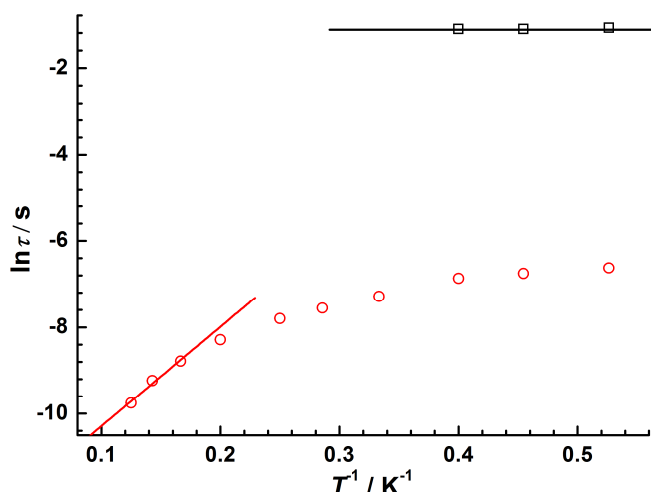


Fig. S14 Plot of relaxation time (τ , natural logarithmic scale) vs. temperature (reciprocal scale) for **2** extracted from frequency-dependent data between 1.9 and 8 K by fitting the χ'' vs. frequency curves. Red circles and black squares refer to the high and low frequency peaks, respectively. The red line represents a linear fit to the Arrhenius equation, affording an effective energy barrier 16 K and pre-exponential factors (τ_0) of 3.4×10^6 .